Three-Body Recombination near a Narrow Feshbach Resonance in ^{6}Li

Jiaming Li,[1,2] Ji Liu,[2] Le Luo,[1,2,*] and Bo Gao[3,†]
[1]School of Physics and Astronomy and Tianqin Research Center for Gravitational Physics, Sun Yat-Sen University, Zhuhai, Guangdong 519082, China
[2]Department of Physics, Indiana University Purdue University Indianapolis, Indianapolis, Indiana 46202, USA
[3]Department of Physics and Astronomy, Mailstop 111, University of Toledo, Toledo, Ohio 43606, USA

(Received 3 January 2018; published 10 May 2018)

We experimentally measure and theoretically analyze the three-atom recombination rate, L_3, around a narrow s-wave magnetic Feshbach resonance of ^{6}Li-^{6}Li at 543.3 G. By examining both the magnetic field dependence and, especially, the temperature dependence of L_3 over a wide range of temperatures from a few μK to above 200 μK, we show that three-atom recombination through a narrow resonance follows a universal behavior determined by the long-range van der Waals potential and can be described by a set of rate equations in which three-body recombination proceeds via successive pairwise interactions. We expect the underlying physical picture to be applicable not only to narrow s wave resonances, but also to resonances in nonzero partial waves, and not only at ultracold temperatures, but also at much higher temperatures.

DOI: 10.1103/PhysRevLett.120.193402

Molecule formation through three-body recombination is one of the most fundamental chemical reactions as it pertains to the very origin of molecules [1,2] and their relative concentration to atomic species. It is also the key to understanding the initial stages of condensation where atoms form molecules which further recombine with other atoms or molecules to grow into bigger molecules, clusters, and, eventually, to mesoscopic and macroscopic objects. As a reflection of the fundamental difficulties in quantum few-body systems, progress on three-body recombination has been excruciatingly slow. Fundamental questions such as the relative importance of direct (background or nonresonant) and indirect (successive pairwise or resonant) processes [3,4] seem as fresh as they were decades ago [5,6]. Unlike deeply bound few-body bound states, for which large basis expansion works to a degree (see, e.g., [7]), three-body recombination occurs at much higher energies around the three-body breakup threshold where the number of open channels for most atoms other than helium goes to practically infinite, making standard numerical methods [8] impractical.

Cold-atom experiments have provided the experimental background for breakthroughs in few-body physics. In such experiments, two-body interaction can be precisely controlled via a Feshbach resonance (FR) [9], and remarkably, manifestations of three-body recombination have become one of the most routinely measured quantities through trap loss. The vast amount of data thus generated has enabled considerable progress in few-body physics, first, in elucidating the Efimov universality [10–13] and, more recently, in discovery and exploration of the van der Waals universality (see, e.g., Refs. [14–20]). Still, much of the progress has, so far, been limited to the zero temperature, to broad s-wave FR's, and to the Efimov regime where the s-wave scattering lengths among the interacting particles are much greater than the ranges of interactions as measured by their corresponding van der Waals length scales. While experiments in other regimes are possible (see, e.g., Refs. [21,22]), they have not received as much attention partly due to the scarcity of the corresponding theories. Further theoretical progress, as well as exciting experimental developments such as state-to-state measurements [23], promise much further progress in few-body physics and chemistry.

In this Letter, first, we reassert that universal behaviors for few-atom and many-atom systems exist much beyond the zero temperature and beyond the s wave, as first suggested some years ago [24]. They exist to the 1-K regime similar to the corresponding quantum-defect theory (QDT) for two-body interactions [25,26] and can be further extended to greater temperature regimes through multiscale QDT [27]. Such broader-sense van der Waals universal behaviors can be mathematically rigorously defined in a way similar to the definitions of universal equations of states at the van der Waals length scale [28–30]. They will be investigated as a part of a QDT for few-atom and many-atom systems. By expanding the region of universal behavior beyond the zero temperature and beyond a broad s-wave resonance, one will, finally, make the connection between studies of idealized few-body systems and real chemistry [2–6,8]. We take a step in this direction here by experimentally measuring and theoretically analyzing the three-atom recombination around a narrow s-wave magnetic FR of ^{6}Li-^{6}Li around 543.3 G. We show that, at ultracold, but finite, temperatures, three-body recombination is dominated by the indirect process if there exists a narrow resonance within k_BT above the threshold. Further, we show that the rate constant describing this

successive pairwise process follows a universal behavior determined by the long-range van der Waals potential. An analytic formula is presented for the rate constant describing both its dependence on the temperature and its dependence on the resonance position, which, in our case, is tunable via a magnetic field.

Experiment.—We prepare a gas of ^{6}Li atoms in the two lowest hyperfine states of $F = 1/2$, $m_F = \pm 1/2$ [labeled as a $(+1/2)$ and b $(-1/2)$ states, respectively] in a magneto-optical trap. The precooled atoms are then transferred into a crossed-beam optical dipole trap made by a fiber laser with 100 watt output. The bias magnetic field is quickly swept to 330 G to implement evaporative cooling [31,32]. A noisy radio-frequency pulse is then applied to prepare a 50:50 spin mixture. At 330 G, the trap potential can be lowered down to 0.1% of the full trap depth (the full trap depth is around 5.6 mK) to obtain a degenerate Fermi gas. After that, the magnetic field is swept well above the narrow FR at 550 G to calibrate the temperature and the initial atom number N_0. Here, the s-wave scattering length of the $a-b$ state is close to the background scattering length of approximately $0.96\beta_6$, for which the gas is weakly interacting [here, $\beta_6 \coloneqq (2\mu C_6/\hbar^2)^{1/4}$ is the van der Waals length scale for ^{6}Li-^{6}Li interaction [25]]. The temperature of a weakly interacting Fermi gas is then measured by fitting the 1D density profile with a finite temperature Thomas-Fermi distribution [33]. To study the temperature dependence of the three-body recombination rate, atom clouds are prepared in a temperature range between 4 and 225 μK by controlling the final trap depth and the evaporative cooling time.

To study the three-body recombination rate around the narrow FR at 543.3 G, the magnetic field is fast swept from 550 G to a target field B_t near the narrow resonance, where we hold the atom cloud for a time duration t. With techniques such as recording the real-time magnets current to monitor the fluctuation of the magnetic field, a field resolution of better than 0.09 G is achieved for all of our data sets. (See the Supplemental Material [34].) After the holding period, the number of atoms left in the trap, $N(t)$, and the Gaussian widths of the cloud, $\sigma_{x(y,z)}$, are extracted from the 2D column density of the absorption images. To avoid the high column density induced error of the atom number, we turn off the optical trap after the holding period and take the absorption images of time-of-flight clouds.

Our atomic vapor is a two-component thermal gas with N_a atoms in state a and N_b atoms in state b. If the densities for atoms in states a and b start out the same, they will remain the same, namely $n_a = n_b =: n$, and decay with the same rate, by

$$\frac{dn}{dt} = -L_3 n^3, \tag{1}$$

where L_3 is the three-body recombination rate. The total atom number $N_a = N_b =: N$ is determined by integrating the density of the whole cloud, where we assume the profile is a Gaussian of the form $n(x,y,z) = n_0 \exp[-x^2/(2\sigma_x^2) - y^2/(2\sigma_y^2) - z^2/(2\sigma_z^2)]$ with n_0 being the atom density at the center of the cloud. The integration gives us

$$\frac{dN(t)}{dt} = -\frac{L_3}{(2\sqrt{3}\pi)^3\sigma_x^2\sigma_y^2\sigma_y^2} N^3(t), \tag{2}$$

implying that $1/N^2$ has a linear dependence on the holding time t with

$$\frac{1}{N^2(t)} = \frac{2L_3}{(2\sqrt{3}\pi)^3\sigma_x^2\sigma_y^2\sigma_y^2} t + \frac{1}{N^2(0)}. \tag{3}$$

By fitting experimental $1/N^2$ to Eq. (3), we extract L_3. (See the Supplemental Material [34].)

We measure L_3 as a function of the magnetic field at various temperatures from 4.2 to 225 μK. They range from at least one Fermi temperature T_F to well above T_F and are all in the thermal gas regime. (See the Supplemental Material [34].) The results are shown in Fig. 1, and will be compared with theory.

Theory.—Our theory describes three-body recombination in a thermal gas and via a narrow resonance as an indirect, successive pairwise process. A narrow resonance can be treated as a bound molecular state weakly coupled to a continuum. The time evolution of atomic number densities, n_a and n_b for atoms in states a and b, respectively, and the number density n_{ab} of metastable molecules in the resonance state $(ab)_r$, are described by a set of rate equations

$$\frac{dn_a}{dt} = +(\Gamma_r/\hbar)n_{ab} - K_{ab}n_a n_b - K_{AD}^M n_a n_{ab} + K_{AD}^B n_a n_{ab} + K_{AD}^B n_b n_{ab}, \tag{4a}$$

$$\frac{dn_b}{dt} = +(\Gamma_r/\hbar)n_{ab} - K_{ab}n_a n_b - K_{AD}^M n_b n_{ab} + K_{AD}^B n_b n_{ab} + K_{AD}^B n_a n_{ab}, \tag{4b}$$

$$\frac{dn_{ab}}{dt} = -(\Gamma_r/\hbar)n_{ab} + K_{ab}n_a n_b - K_{AD}n_a n_{ab} - K_{AD}n_b n_{ab}. \tag{4c}$$

Here, Γ_r is the width of the resonance. K_{ab} is the rate for the formation of metastable molecules via two-body collision at temperature T. It is related to the resonance width Γ_r by

$$K_{ab} = (\Gamma_r/\hbar)(\sqrt{2}\lambda_T)^3(2l_r+1)e^{-\epsilon_r/k_BT}, \tag{5}$$

for a resonance in partial wave l_r located at energy ϵ_r. Here, $\lambda_T \coloneqq (2\pi\hbar^2/mk_BT)^{1/2}$ is the thermal wave length of an atom at temperature T. The K_{AD}^M in Eq. (4) is the rate of

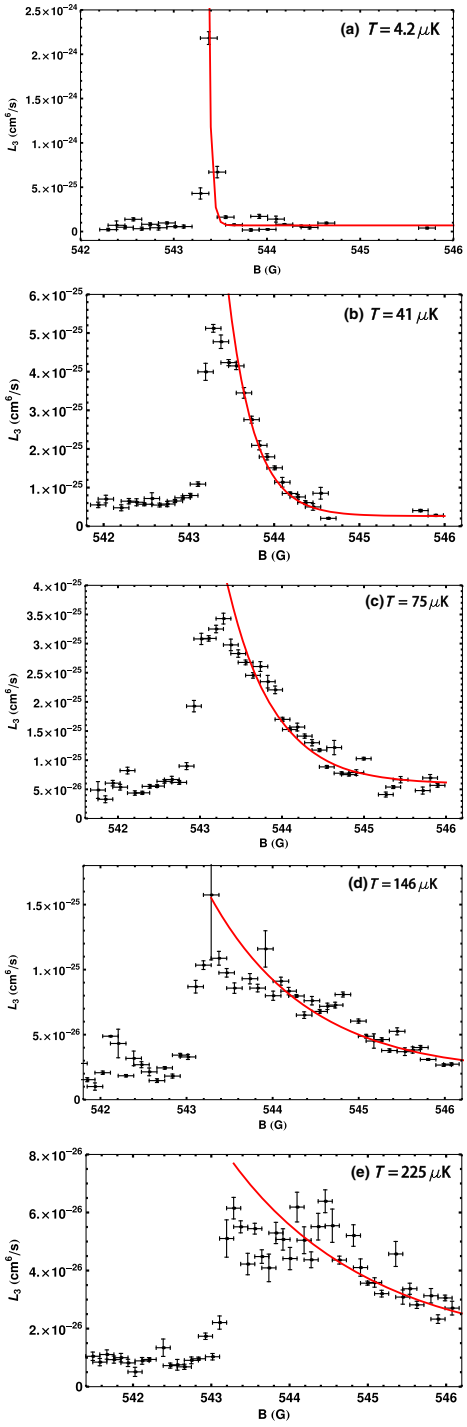

FIG. 1. $L_3(T,B)$ as a function of the magnetic field B at temperatures 4.2 μK (a), 41 μK (b), 75 μK (c), 146 μK (d), 225 μK (e). The red lines are the fits to theory to be discussed later. The magnetic FR crosses the threshold at $B_0 = 543.25$ G. The trap losses for $B < B_0$ are due to higher-order processes that are not considered in this Letter.

atom-dimer interaction leading to the formation of a stable molecule, namely for the processes of $a + (ab)_r \to a + (ab)_M$ and $a + (ab)_r \to b + (aa)_M$, or $b + (ab)_r \to b + (ab)_M$ and $b + (ab)_r \to a + (bb)_M$. K^B_{AD} is the rate of breakup of a metastable molecule via $a + (ab)_r \to 2a + b$ or $b + (ab)_r \to a + 2b$. $K_{AD} = K^M_{AD} + K^B_{AD}$ is the total inelastic and reactive rate for atom-dimer interaction. This rate equation ignores the contribution from the direct three-body process to focus on the contribution from the indirect process, which will be shown later to dominate at cold temperatures.

The seemingly complex rate equation, Eq. (4), simplifies if the Γ_r and the time of measurement have allowed n_{ab} to reach a steady state, characterized by $dn_{ab}/dt = 0$. In the steady state, one obtains

$$n_{ab} = \frac{(\Gamma_r/\hbar)}{(\Gamma_r/\hbar) + K_{AD}(n_a + n_b)} 2^{3/2}\lambda_T^3(2l_r + 1)e^{-\epsilon_r/k_BT}. \quad (6)$$

Under the further initial condition of $n_a(t=0) = n_b(t=0)$, corresponding to our experiment, and the condition of $\Gamma_r/\hbar \gg K_{AD}(n_a + n_b)$, we obtain, in steady state, $n_a(t) = n_b(t) =: n(t)$ and satisfy Eq. (1) with L_3 given by

$$L_3(T,\epsilon_r) = 3K^M_{AD}(T,\epsilon_r)(\sqrt{2}\lambda_T)^3(2l_r + 1)e^{-\epsilon_r/k_BT}. \quad (7)$$

All the required conditions are well satisfied in our experiment. We caution, however, that the typical three-body rate equation, Eq. (1), should not be taken for granted for indirect processes. They can have other behaviors under different conditions.

Through Eq. (7), the rate equation, Eq. (4), reduces the understanding of L_3 to the understanding of K^M_{AD} which is the rate for the formation of bound molecules in atom interaction with a metastable dimer. This bimolecular process differs from the typical atom-(truly bound) dimer interaction in that its inelastic component does not always lead to the formation of bound molecules even in the limit of zero atom-dimer energy. It can also lead to the breakup of the metastable dimer, resulting in three free atoms. Our theory for K^M_{AD} is based on the multichannel quantum defect theory for reactions and inelastic processes as outlined in Ref. [35]. Following an analysis similar to what led to the quantum Langevin (QL) model for reactions [35,36], we obtain

$$K^M_{AD}(T,\epsilon_r) = s^{AD}_K \frac{2}{\sqrt{\pi}} \int_0^\infty dx x^{1/2} e^{-x} \times \sum_{l=0}^{\infty} \mathcal{M}_{l_r l}(\epsilon_r + k_BTx)\mathcal{W}^{(6)}_{\mathrm{url}}(T_s x). \quad (8)$$

Here, s^{AD}_K is the rate scale for atom-dimer interaction with a van der Waals $-C^{AD}_6/R^6$ long range potential. More specifically, $s^{AD}_K := \pi\hbar\beta^{AD}_6/\mu^{AD}$, where μ^{AD} is the atom-dimer reduced mass and $\beta^{AD}_6 := (2\mu^{AD}C^{AD}_6/\hbar^2)^{1/4}$ is the length scale associated with the atom-dimer van der Waals potential. $\mathcal{M}_{l_r l}(\epsilon_f = \epsilon_r + \epsilon_{AD}) := \sum_{f\in M}|(S^c_{\mathrm{eff}})_{fi}|^2$ is a short-range branching ratio for transitions into bound

molecular states characterized by set $\{M\}$, with $S^c_{\rm eff}$ being the effective short-range S matrix characterizing atom-dimer, namely three-body interaction within the range of the van der Waals length scale [25,35]. $\mathcal{W}^{(6)}_{{\rm url}}(\epsilon_s)$ is the universal partial inelastic and reactive QL rate for partial wave l [35]. $T_s := T/s^{AD}_T$ is a scaled temperature, with s^{AD}_T being the temperature scale given by $s^{AD}_T := s^{AD}_E/k_B$ where $s^{AD}_E := (\hbar^2/2\mu^{AD})(1/\beta^{AD}_6)^2$ is the energy scale associated with β^{AD}_6.

Equations (7) and (8) provide a foundation for understanding the universal behaviors of three-body recombination via a narrow resonance over a wide range of energies and temperatures. We focus, here, on an s-wave resonance ($l_r = 0$) and on the ultracold temperature regime of $T \ll s^{AD}_T$ (namely $T_s \ll 1$), to derive an analytic formula for L_3 that is most useful in current experiments. Using the unitarity of an S matrix, we can write $\mathcal{M}_{l_r l}(\epsilon_f) = 1 - \sum_{f\in B}|(S^c_{\rm eff})_{fi}|^2$, namely in terms of the short-range branching ratio into the three-body breakup channels $\{B\}$. Taking advantage of the short-range S matrix being insensitive to energy and angular momenta [25,37], the short-range branching ratio to bound molecular states is approximately a constant $\mathcal{M}_{l_r=0 l=0}(\epsilon_f) \approx \mathscr{M}$ with $\mathscr{M}$ being a dimensionless three-body parameter related to $S^c_{\rm eff}$ and constrained by $0 < \mathscr{M} \le 1$. Substituting this result into Eq. (8), we obtain for an s-wave resonance ($l_r = 0$) in the ultracold region of $T \ll s^{AD}_T$

$$K^M_{AD}(T, \epsilon_r) \approx \mathscr{M} K^{{\rm QL}(6)}_{AD}(T_s), \tag{9}$$

with $K^{{\rm QL}(6)}_{AD}(T_s)$ being the universal QL rate that is well approximated in the ultracold s-wave region by [35]

$$K^{{\rm QL}(6)}_{AD}(T_s) \approx s^{AD}_K 4\bar{a}^{(6)}_{sl=0}\left(1 - \frac{4\bar{a}^{(6)}_{sl=0}}{\sqrt{\pi}} T_s^{1/2}\right), \tag{10}$$

where $\bar{a}^{(6)}_{sl=0} = 2\pi/[\Gamma(1/4)]^2 \approx 0.477\,988\,8$ is a universal number that represents the scaled mean s-wave scattering length for a $-1/R^6$-type van der Waals potential [38].

Substituting Eq. (9) into Eq. (7), we obtain

$$L_3(T, \epsilon_r) \approx 3\mathscr{M} K^{{\rm QL}(6)}_{AD}(T_s)(\sqrt{2}\lambda_T)^3 e^{-\epsilon_r/k_B T}. \tag{11}$$

In the presence of a narrow s-wave resonance within an ultracold energy range of the order of $k_B T$ above the threshold, Eq. (11) gives an analytic description of the three-body recombination rate L_3 as a function of both the temperature and the resonance position, in terms of a single dimensionless three-body parameter $0 < \mathscr{M} \le 1$. The resonance can, in principle, be of any origin, but a magnetic FR offers a unique opportunity to tune the resonance position and, thus, to test the predicted dependence on ϵ_r.

TABLE I. The measured results and error bars of $K^M_{AD}(T)$

T (μK)	δT (μK)	K^M_{AD} (10^{-10} cm^3/s)	δK^M_{AD} (10^{-12} cm^3/s)
4.2	0.2	1.04	8
41	4	0.878	7
75	4	0.803	6
146	7	0.794	6
225	11	0.720	5

Comparison between theory and experiment.—For ^{6}Li, using $C_6 = 1393.39$ a.u. [39] for the atom-atom potential, we have $C^{AD}_6 \approx 2C_6 = 2786.78$ a.u., from which we have $\beta^{AD}_6 = 79.8935$ a.u., $s^{AD}_T = 3383.85$ μK, and $s^{AD}_K = 2.1035 \times 10^{-10}$ cm^3/s. For our particular Feshbach resonance, the resonance position is given by $\epsilon_r = \mu_r(B - B_0)$ with $\mu_r = 1.98\mu_B$ being the differential magnetic moment for the resonance [9]. Equation (7) now gives us

$$L_3(T, B) \approx 3K^M_{AD}(T)(\sqrt{2}\lambda_T)^3 \exp\left[-\frac{\mu_r(B - B_0)}{k_B T}\right]. \tag{12}$$

Figure 1 shows the fits of this equation to experimental loss spectra, giving experimental results of $K^M_{AD}(T)$ at five different temperatures, tabulated in Table I and plotted in Fig. 2. Our result for K^M_{AD} at the lower end of the temperatures, 4.2 μK, is consistent with the earlier result of Hazlett *et al.* [21]. Figure 2 further shows that the temperature dependence of the rate $K^M_{AD}(T)$ is well described by analytic formulas, Eqs. (9) and (10), a fit to which gives us the three-body parameter $\mathscr{M} = 0.25 \pm 0.01$, consistent with $0 < \mathscr{M} \le 1$.

Discussions and conclusions.—We have measured and analyzed three-body recombination around a narrow s-wave resonance and in a thermal gas regime. The resonance is much narrower than $k_B T$ and is located in a

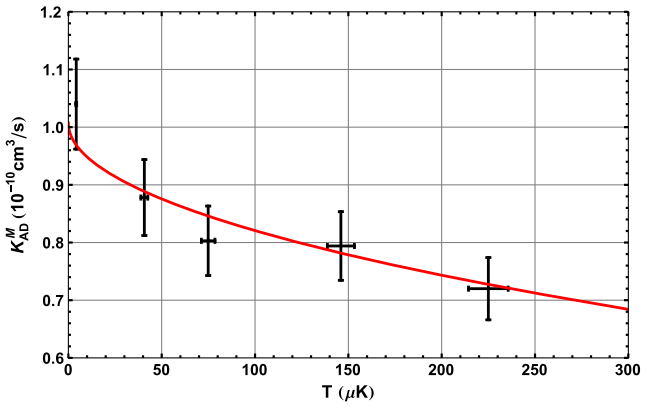

FIG. 2. The rate constant $K^M_{AD}(T)$ near the ^{6}Li narrow s-wave FR resonance at 543.25 G. The red solid line is a fit of our theoretical model, Eqs. (9) and (10), to our experimental measurements from which the three-body parameter $\mathscr{M} = 0.25 \pm 0.01$ is extracted.

neighborhood of $k_B T$ above the threshold. We have shown that the recombination follows a universal behavior determined by the van der Waals potential with a single three-body parameter $\mathscr{M}$. When applied to a magnetic FR, the theory gives the line shape of the Feshbach spectrum, namely L_3 vs B, described by Eq. (12). It shows that the line shape is temperature-dependent and has a width of the order of $k_B T/\mu_B$ (see, also, Ref. [21]). Other than the details of $\mathscr{M}$, the results are equally applicable to identical bosons and easily generalized to other cases.

The theory further shows that, in the presence of a narrow s-wave resonance within $k_B T$ above the threshold, the indirect process has a rate of the order $(\hbar/m)\beta_6\lambda_T^3$, which, at ultracold temperatures of $T \ll s_T$, is much greater than those for the direct processes. For bosons, it is greater by a factor of $(\lambda_T/\beta_6)^3$ since the direct process has a rate of the order $(\hbar/m)\beta_6^4$ [40,41]. The enhancement factor is even greater, by another (s_T/T), for our two-component fermion case for which the direct process has a rate of the order $(\hbar/m)\beta_6^4(T/s_T)$ [40,41]. Thus, at ultracold temperatures, the indirect process dominates the three-body recombination if there is a narrow s-wave resonance within $k_B T$ above the threshold.

Many of the concepts of this work are applicable to resonances in nonzero partial waves (see, e.g., Refs. [42–45]), the understanding of which will further expand the temperature regime of three-body physics towards practical chemistry [2–6,8]. More measurements of $\mathscr{M}$ for other narrow resonances and other systems will further stimulate a deeper understanding of this three-body parameter. It can be expected to be related in a universal manner to short-range K^c matrix parameters K_S^c and K_T^c for atom-atom interaction in (electronic) spin singlet and triplet, respectively [26]. Such a relationship, when revealed and understood, would signal the arrival of a QDT for few-atom systems, and will represent a big step forward in few-body physics and in chemistry.

L. L. received support from Indiana University IUCRG, RSFG, Purdue University PRF, Grant No. CNSF-11774436. B. G. is supported by NSF under Grant PHY-1607256.

*Also at the Indiana University Center for Spacetime Symmetries (IUCSS).
leluo@iupui.edu
†bo.gao@utoledo.edu

[1] M. J. Turk, P. Clark, S. C. O. Glover, T. H. Greif, T. Abel, R. Klessen, and V. Bromm, Astrophys. J. **726**, 55 (2011).
[2] R. C. Forrey, Astrophys. J. Lett. **773**, L25 (2013).
[3] J. Prez-Ros, S. Ragole, J. Wang, and C. H. Greene, J. Chem. Phys. **140**, 044307 (2014).
[4] R. C. Forrey, J. Chem. Phys. **143**, 024101 (2015).
[5] G. W. Wei, S. Alavi, and R. F. Snider, J. Chem. Phys. **106**, 1463 (1997).
[6] R. T Pack, R. B. Walker, and B. K. Kendrick, J. Chem. Phys. **109**, 6701 (1998).
[7] Y. Suzuki and K. Varga, *Stochastic Variational Approach to Quantum-Mechanical Few-Body Problems* (Springer-Verlag, Berlin, 1998).
[8] H. Suno, B. D. Esry, C. H. Greene, and J. P. Burke, Jr, Phys. Rev. A **65**, 042725 (2002).
[9] C. Chin, R. Grimm, P. Julienne, and E. Tiesinga, Rev. Mod. Phys. **82**, 1225 (2010).
[10] E. Nielsen, D. Fedorov, A. Jensen, and E. Garrido, Phys. Rep. **347**, 373 (2001).
[11] E. Braaten and H.-W. Hammer, Phys. Rep. **428**, 259 (2006).
[12] T. Kraemer, M. Mark, P. Waldburger, J. G. Danzl, C. Chin, B. Engeser, A. D. Lange, K. Pilch, A. Jaakkola, H.-C. Nägerl, and R. Grimm, Nature (London) **440**, 315 (2006).
[13] C. H. Greene, Phys. Today **63**, No. 3 40 (2010).
[14] M. Berninger, A. Zenesini, B. Huang, W. Harm, H.-C. Nägerl, F. Ferlaino, R. Grimm, P. S. Julienne, and J. M. Hutson, Phys. Rev. Lett. **107**, 120401 (2011).
[15] J. Wang, J. P. D'Incao, B. D. Esry, and C. H. Greene, Phys. Rev. Lett. **108**, 263001 (2012).
[16] Y. Wang, J. Wang, J. P. D'Incao, and C. H. Greene, Phys. Rev. Lett. **109**, 243201 (2012).
[17] P. Naidon, S. Endo, and M. Ueda, Phys. Rev. Lett. **112**, 105301 (2014).
[18] D. Blume, Few-Body Syst. **56**, 859 (2015).
[19] P. M. A. Mestrom, J. Wang, C. H. Greene, and J. P. D'Incao, Phys. Rev. A **95**, 032707 (2017).
[20] J. Johansen, B. J. DeSalvo, K. Patel, and C. Chin, Nat. Phys. **13**, 731 (2017).
[21] E. L. Hazlett, Y. Zhang, R. W. Stites, and K. M. O'Hara, Phys. Rev. Lett. **108**, 045304 (2012).
[22] T. T. Wang, M.-S. Heo, T. M. Rvachov, D. A. Cotta, and W. Ketterle, Phys. Rev. Lett. **110**, 173203 (2013).
[23] J. Wolf, M. Deiß, A. Krükow, E. Tiemann, B. P. Ruzic, Y. Wang, J. P. D'Incao, P. S. Julienne, and J. H. Denschlag, Science **358**, 921 (2017).
[24] B. Gao, J. Phys. B **36**, 2111 (2003).
[25] B. Gao, Phys. Rev. A **78**, 012702 (2008).
[26] B. Gao, E. Tiesinga, C. J. Williams, and P. S. Julienne, Phys. Rev. A **72**, 042719 (2005).
[27] H. Fu, M. Li, M. K. Tey, L. You, and B. Gao, New J. Phys. **18**, 103016 (2016).
[28] B. Gao, J. Phys. B **37**, L227 (2004).
[29] B. Gao, Phys. Rev. Lett. **95**, 240403 (2005).
[30] I. Khan and B. Gao, Phys. Rev. A **73**, 063619 (2006).
[31] J. Li, J. Liu, W. Xu, L. de Melo, and L. Luo, Phys. Rev. A **93**, 041401 (2016).
[32] J. Li, L. de Melo, and L. Luo, J. Vis. Exp. **121**, e55409 (2017).
[33] L. Luo, Ph.D. thesis, Duke University, 2008.
[34] See Supplemental Material at http://link.aps.org/supplemental/10.1103/PhysRevLett.120.193402 for further experimental details.
[35] B. Gao, Phys. Rev. Lett. **105**, 263203 (2010).
[36] B. Gao, Phys. Rev. A **83**, 062712 (2011).
[37] B. Gao, Phys. Rev. A **64**, 010701 (2001).
[38] B. Gao, Phys. Rev. A **80**, 012702 (2009).

[39] Z.-C. Yan, J. F. Babb, A. Dalgarno, and G. W. F. Drake, Phys. Rev. A **54**, 2824 (1996).
[40] B. D. Esry, C. H. Greene, and H. Suno, Phys. Rev. A **65**, 010705 (2001).
[41] J. P. D'Incao and B. D. Esry, Phys. Rev. Lett. **94**, 213201 (2005).
[42] C. A. Regal, C. Ticknor, J. L. Bohn, and D. S. Jin, Phys. Rev. Lett. **90**, 053201 (2003).
[43] C. Ticknor, C. A. Regal, D. S. Jin, and J. L. Bohn, Phys. Rev. A **69**, 042712 (2004).
[44] Y. Cui, C. Shen, M. Deng, S. Dong, C. Chen, R. Lü, B. Gao, M. K. Tey, and L. You, Phys. Rev. Lett. **119**, 203402 (2017).
[45] X.-C. Yao, R. Qi, X.-P. Liu, X.-Q. Wang, Y.-X. Wang, Y.-P. Wu, H.-Z. Chen, P. Zhang, H. Zhai, Y.-A. Chen, and J.-W. Pan, arXiv:1711.06622.

Supplementary material for "Three-body recombination near a narrow Feshbach resonance in ^{6}Li"

Jiaming Li,[1,2] Ji Liu,[2] Le Luo,[1,2] and Bo Gao[3]

[1]*School of Physics and Astronomy and Tianqin Research Center for Gravitational Physics, Sun Yat-Sen University, Zhuhai, Guangdong, China 519082*
[2]*Department of Physics, Indiana University Purdue University Indianapolis, Indianapolis, IN 46202*
[3]*Department of Physics and Astronomy, Mailstop 111, University of Toledo, Toledo, OH 43606*

TIME-DEPENDENT ATOM LOSS

The 3-body loss rate L_3 is obtained by fitting the time-dependent atom number with Eq. (3) in the main text. The time-dependent atom number is expressed in the form of $1/N^2(t)$ so that the fitting formula is a linear function, the slope of which gives L_3. A typical time-dependent atom number data is shown in Fig. 1.

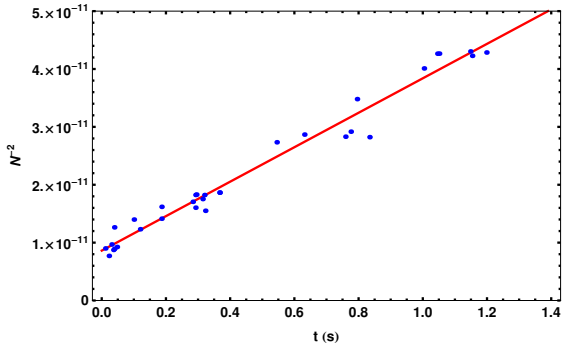

FIG. 1: The time-dependent $1/N^2$ where N is the atom number left in the optical trap. The data is taken for a 70 μK cloud at the magnetic field 543.9 G. The fitting gives $L_3 = 2.455 \times 10^{-25}$ cm^6/s.

TEMPERATURE OF THE ATOM CLOUD

To measure the rate constant $K_{AD}^M(T)$ around the ^{6}Li narrow s-wave Feshbach resonance at 543.3 G, it is highly desired that the range of the temperature measured is as large as possible. However, there are constrains in both the high temperature limit and the low temperature limit. It is noted that we want to be in the thermal gas regime for this work. So we intentionally avoid temperatures well below the Fermi temperature. Also, the resonance profile becomes very narrow, close to 0.1 G [1], when the temperature is less than the Fermi temperature, while in our current setup the magnetic field resolution is only about 0.09 G (the equivalent standard derivation is about 0.05 G). So we choose several μK as the low end of the temperature. For the high temperature data, we reduce the evaporative cooling time and use the deep trap to hold the hot atom cloud. However, the deeper trap requires higher power of the trapping beam which results in additional heating and loss and limits the availability of the high temperature data. We choose the highest temperature of about 200 μK, where the trap has at least 15 second lifetime for a noninteracting Fermi gas at 528 G.

The trapping parameters of our data set at different temperatures are listed in Table I, where $\omega_{x,y,z}$ are frequencies of the trap used to hold the cloud, N_{avg} is the average single spin atom number corresponding to the temperature, and T_F is the Fermi temperature. The data indicate that we are in the thermal gas regime, where the Fermi statistics does not play a significant role.

STABILIZATION AND MEASUREMENT OF THE MAGNETIC FIELD

The resonance width ΔB of the ^{6}Li narrow Feshbach resonance near 543.3 G is about 0.1 G [1]. Experimental studies around this resonance usually requires very high magnetic field resolution well below 0.1 G. Our experimental data are

T (μK)	ω_x ((2πHz)	ω_y (2πHz)	ω_z (2πHz)	N_{avg}	T_F (μK)	T/T_F
4.2	169.0	1590.5	1752.5	221900	4.1	1.0
41	534.2	5028.9	5541.0	297825	14.3	2.9
75	755.5	7112.0	7836.1	358042	21.6	3.5
146	1068.4	10057.8	11082.0	458207	33.1	4.4
225	1510.9	14223.9	15672.2	449510	46.5	4.8

TABLE I: The trapping parameters of the atom clouds at different temperatures.

in the temperature range of several μK to hundreds of μK. These temperatures are well above the Fermi temperature and significantly broaden the resonance profile, which relaxes the constraint of the magnetic field resolution in our experiment. For example, at $T = 41$ μK, $k_BT/\mu_r \approx 0.3$ G, and we need only to have a field resolution smaller than or comparable to 0.3 G.

We adopt several methods to stabilize and precisely determine the magnetic field so that the resolution is less than 0.09 G for all data points. First, we use a passive method to control the magnetic field. The magnetic field is generated by a pair of water-cooled magnetic coils. The efficient water cooling allows the temperature fluctuation of the magnetic coils to be less than 1 °C. The magnetic field is controlled by the current of the coils, which is commanded by an external control voltage. The resolution of the control is 15 ppm (parts per million), which is equivalent to 0.075 G. By continuously commanding the current of the coils, the magnetic field is locked to a certain value, which provide a passive stabilization.

Second, we employ a high accuracy measuring system to record the real-time magnetic field for all data points. The system includes a Keithley ultralow noise autoranging digital multimeter (DMM) and a computer to record the real-time current fluctuation for the whole sequence of every measurement. It should be emphasized that by recording the magnetic field for every measurement, we could repeat the same measurement many times and keep the data that have relatively small magnetic fluctuation for analysis. This helps us to reduce the systematic error induced by the magnetic field fluctuation. A typical measuring curve of the magnetic field fluctuation is presented in Fig. 2.

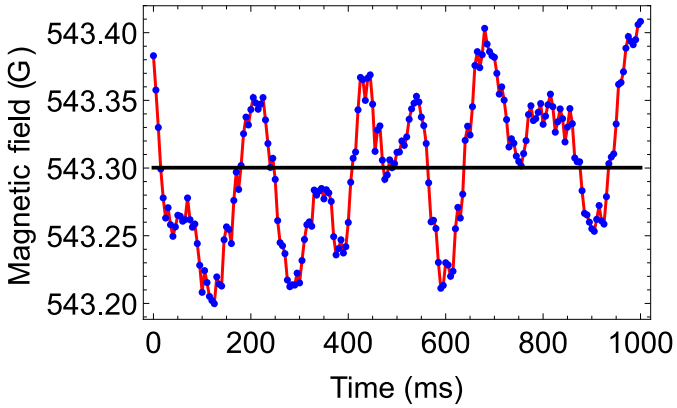

FIG. 2: The magnetic field fluctuation recorded during the holding time of measuring atom loss. The trap is held for 1000 ms, then the residual atom number in the trap is measured. The magnetic field fluctuation during the holding time is recorded while the magnetic field is calculated from the measured current. The standard derivation of the magnetic field is about 0.05 G during the holding time. The sampling rate of the DMM is 200 Hz. The noise level of the DMM is about 10 times smaller than the fluctuation of the magnetic field.

For all the data we present, the standard derivation of the magnetic field is less than 0.05 G, which is represented by the error bar of the magnetic field shown in Fig. 2 of the main text.

[1] C. Chin, R. Grimm, P. Julienne, and E. Tiesinga, Rev. Mod. Phys. **82**, 1225 (2010).